Computed tomography (CT)

Part 2

André Sopczak

Institute of Experimental and Applied Physics,
Czech Technical University in Prague
http://cern.ch/sopczak
andre.sopczak@cvut.cz
based on lectures 2005-2022 by Jan Kybic,
Department of Cybernetics, FEE CTU

2023

Analytical methods

Algebraic reconstruction

3D CT

Radiation dose

Reconstruction methods

- *Backprojection* (not an inverse)
- *Fourier reconstruction* (slow)
- Filtered backprojection
- Algebraic reconstruction (iterative)

Forward projection

sinogram

$$P_\varphi(r) = \int_{(x,y)\in L(r,\varphi)} \mu(x,y)\mathrm{d}l$$

$$r = x\cos\varphi + y\sin\varphi$$

$$P_\varphi(r) = \int_t o(x,y)\mathrm{d}t$$

$$x = r\cos\varphi - t\sin\varphi$$

$$y = r\sin\varphi + t\cos\varphi$$

Variable correspondence:

$$\xi' = r, \quad \eta' = t, \quad \xi = x, \quad \eta = y$$

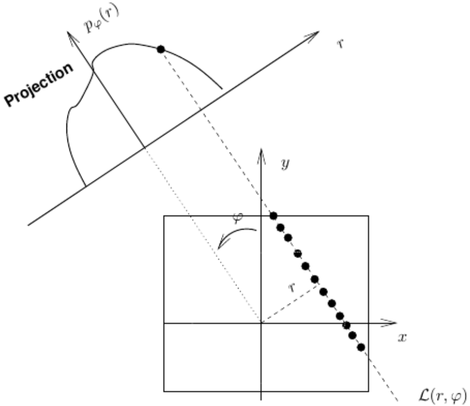

Backprojection

laminogram

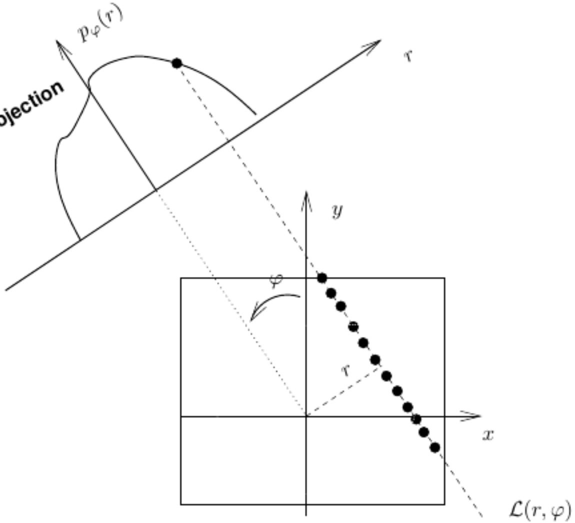

Backprojection
laminogram

$$\mu_b(x, y) = \int_0^\pi P_\varphi(r)\mathrm{d}\varphi$$
$$r = x\cos\varphi + y\sin\varphi$$

for uniformly discretized φ

$$\varphi_i = \pi(i-1)/n_\varphi, \quad i = 1, \dots, n_\varphi$$
$$\mu_b(x, y) \approx \frac{\pi}{n_\varphi}\sum_{i=1}^{n_\varphi} P_\varphi(x\cos\varphi_i + y\sin\varphi_i)$$

Backprojection

. . . is **not** an inverse of the Radon transform, leads to *star artifacts*

laminogram μ_b — the original object μ blurred, convolved by $1/|r|$

Backprojection

...is **not** an inverse of the Radon transform, leads to *star artifacts*

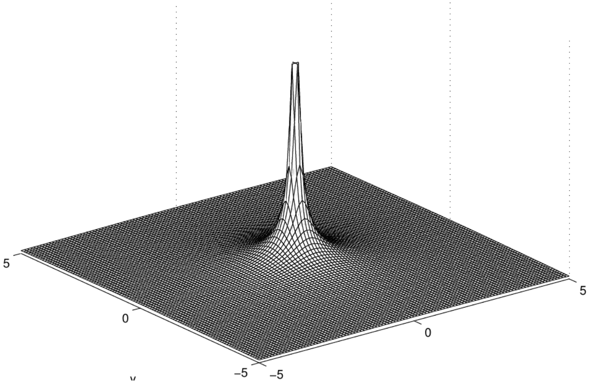

laminogram μ_b — the original object μ blurred, convolved by $1/|r|$

Central slice theorem

(Projection Theorem, Věta o centrálním řezu)

$$P_\varphi(r) = \int \mu(r\cos\varphi - t\sin\varphi, r\sin\varphi + t\cos\varphi)\mathrm{d}t$$

Fourier transform of the Radon transform by r:

$$\begin{aligned}\mathscr{F}\left\{\mathscr{R}\left[\mu(x,y)\right]\right\} = \mathscr{F}\left\{P_\varphi(r)\right\} = \hat{P}_\varphi(\omega) &= \int P_\varphi(r)\mathrm{e}^{-2\pi j\omega r}\mathrm{d}r \\ &= \iint \mu(r\cos\varphi - t\sin\varphi, r\sin\varphi + t\cos\varphi)\mathrm{e}^{-2\pi j\omega r}\mathrm{d}r\mathrm{d}t\end{aligned}$$

Substitution $(r,t) \to (x,y)$:

$$\hat{P}_\varphi(\omega) = \int \mu(x,y)\mathrm{e}^{-2\pi j\omega(x\cos\varphi + y\sin\varphi)}\mathrm{d}x\mathrm{d}y$$

Central slice theorem

$$\hat{P}_\varphi(\omega) = \int \mu(x, y)\mathrm{e}^{-2\pi j\omega(x\cos\varphi + y\sin\varphi)}\mathrm{d}x\mathrm{d}y$$

Denote $u = \omega\cos\varphi \quad v = \omega\sin\varphi$

$$\hat{P}(u, v) = \int \mu(x, y)\mathrm{e}^{-2\pi j(xu+yv)}\mathrm{d}x\mathrm{d}y$$

and therefore

$$\hat{P}(u, v) = \mathscr{F}\left\{\mu(x, y)\right\}$$
$$\hat{P}_\varphi(\omega) = \mathscr{F}\left\{\mu(x, y)\right\}(\omega\cos\varphi, \omega\sin\varphi) = \hat{\mu}(\omega\cos\varphi, \omega\sin\varphi)$$

Central slice theorem

$$\hat{P}(u, v) = \mathscr{F}\left\{\mu(x, y)\right\}$$

$$\hat{P}_\varphi(\omega) = \mathscr{F}\left\{\mu(x, y)\right\}(\omega \cos\varphi, \omega \sin\varphi) = \hat{\mu}(\omega \cos\varphi, \omega \sin\varphi)$$

Slice of the 2D Fourier transform of the image μ at angle φ is the 1D Fourier transform of the projection P_φ of the same image μ.

Fourier reconstruction

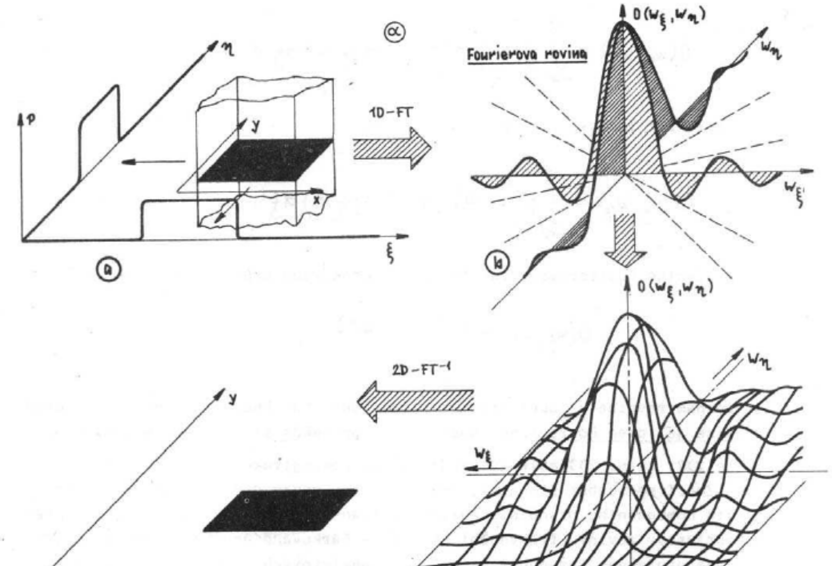

Fourier reconstruction (2)

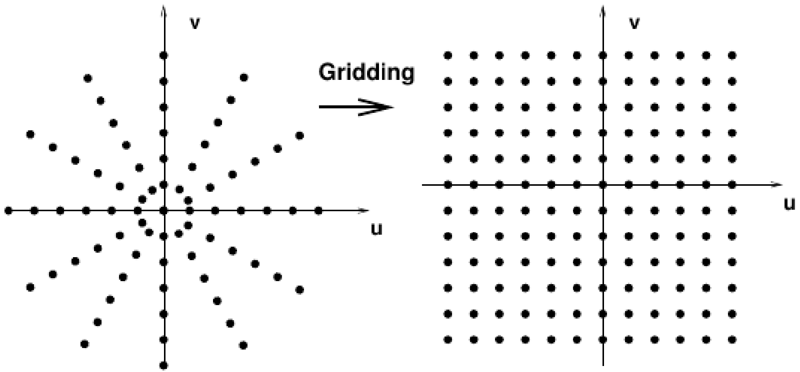

- 1D FT $\hat{P}_\varphi(\omega)$ of each projection $P_\varphi(r)$
- Interpolate FT from polar to Cartesian grid (to get $\hat{P}(u, v)$)
- Inverse 2D FT $\hat{P}(u, v)$ to get object μ

Cons: computational complexity, interpolation artifacts

Inverse Radon transform

From the Fourier slice theorem:

$$\hat{P}(u,v) = \mathscr{F}\left\{\mu(x,y)\right\}$$

$$\mu(x,y) = \mathscr{F}^{-1}\left\{\hat{P}(u,v)\right\} = \int\limits_{-\infty}^{\infty}\int\limits_{-\infty}^{\infty} \hat{P}(u,v)\mathrm{e}^{2\pi j(xu+yv)}\mathrm{d}u\mathrm{d}v$$

Polar coordinates $u = \omega\cos\varphi, \quad v = \omega\sin\varphi$:

$$\mu(x,y) = \int\limits_{0}^{\pi}\int\limits_{-\infty}^{\infty} \hat{P}_{\varphi}(\omega)\mathrm{e}^{2\pi j\omega(x\cos\varphi + y\sin\varphi)}|\omega|\mathrm{d}\omega\mathrm{d}\varphi$$

where $|\omega|$ is the Jacobian (determinant) of $(\omega,\phi) \to (u,v)$

$$\begin{vmatrix} \frac{\partial u}{\partial \varphi} & \frac{\partial u}{\partial \omega} \\ \frac{\partial v}{\partial \varphi} & \frac{\partial v}{\partial \omega} \end{vmatrix} = \left|-\omega\sin^2\varphi - \omega\cos^2\varphi\right| = |\omega|$$

Inverse Radon transform

$$\mu(x, y) = \int_0^{\pi} \int_{-\infty}^{\infty} \hat{P}_\varphi(\omega) \mathrm{e}^{2\pi j \omega (x \cos\varphi + y \sin\varphi)} |\omega| \mathrm{d}\omega \mathrm{d}\varphi$$

can be written as

$$\mu(x, y) = \int_0^{\pi} Q_\varphi(\underbrace{x \cos\varphi + y \sin\varphi}_{r}) \mathrm{d}\varphi$$

$$Q_\varphi(r) = \int_{-\infty}^{\infty} \hat{P}_\varphi(\omega) \mathrm{e}^{2\pi j \omega r} |\omega| \mathrm{d}\omega$$

where $Q_\varphi(r)$ is a modified projection

Inverse Radon transform

$$\mu(x,y) = \int_0^\pi Q_\varphi(r)\mathrm{d}\varphi$$
$$Q_\varphi(r) = \int_{-\infty}^{\infty} \hat{P}_\varphi(\omega)\mathrm{e}^{2\pi j\omega r}|\omega|\mathrm{d}\omega$$
$$Q_\varphi(r) = \mathscr{F}^{-1}\left\{|\omega|\hat{P}_\varphi(\omega)\right\} = \mathscr{F}^{-1}\left\{|\omega|\right\} * P_\varphi(r)$$

defining the exact inverse Radon transform

$$P_\varphi(r) = \mathscr{R}\left[\mu(x,y)\right]$$
$$\mu(x,y) = \mathscr{R}^{-1}\left[P_\varphi(r)\right]$$

Filtered backprojection

Filtrovaná zpětná projekce

- Filter all projections $P_\varphi(r)$ for all φ, get modified projections $Q_\varphi(r)$
- Backproject modified projections and sum

$$\mu(x,y) = \int_0^\pi Q_\varphi(r)\mathrm{d}\varphi$$

$$Q_\varphi(r) = h(t) * P_\varphi(r) = \mathscr{F}^{-1}\{H(\omega)\} * P_\varphi(r)$$

$$H(\omega) = |\omega|$$

- No Fourier transform involved.

Practical implementation of filtered backprojection

- **Problem:** Ideal filter $H(\omega) = |\omega|$ amplifies noise
- **Solution:** Make $\hat{P}_\varphi(\omega)$ frequency limited. Ramakrishnan-Lakshiminaryanan $\longrightarrow$ Ram-Lak filter:

$$H(\omega) = \begin{cases} |\omega| & \text{if } |\omega| \leq \Omega \\ 0 & \textit{otherwise} \end{cases}$$

Practical implementation of filtered backprojection

- **Problem:** Ideal filter $H(\omega) = |\omega|$ amplifies noise
- **Solution:** Make $\hat{P}_\varphi(\omega)$ frequency limited. Ramakrishnan-Lakshiminaryanan $\longrightarrow$ Ram-Lak filter:

$$H(\omega) = \begin{cases} |\omega| & \text{if } |\omega| \leq \Omega \\ 0 & \textit{otherwise} \end{cases}$$

- Ram-Lak filter causes artefacts (Gibbs). Many solutions (Hamming filter, Shepp-Logan filter). Tradeoff between SNR and resolution.

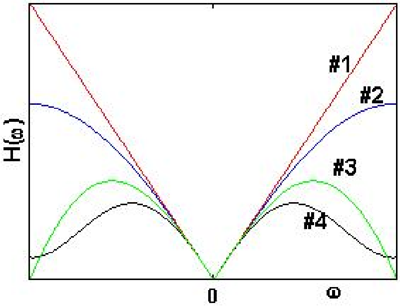

Bandlimited ramp filter h

in space domain

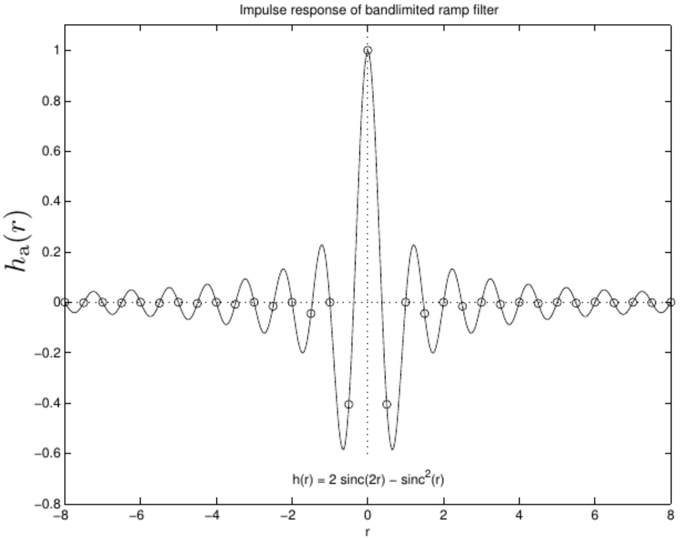

Filtered backprojection example

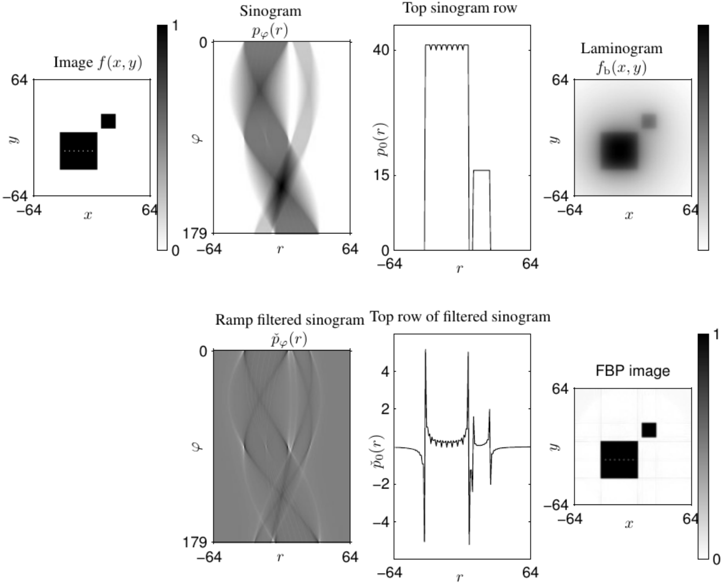

Filtered backprojection

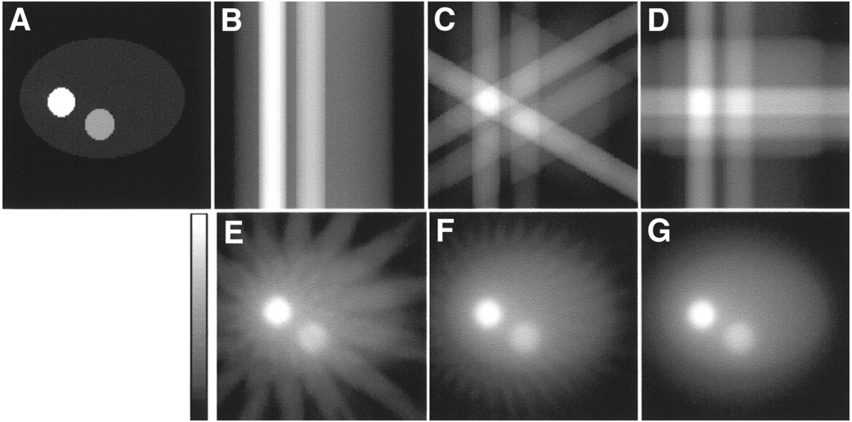

original image, 1,3, 4, 16, 32, a 64 projections

Fan-beam reconstruction

- Rays not parallel, not a Radon transform.
- Rebinning

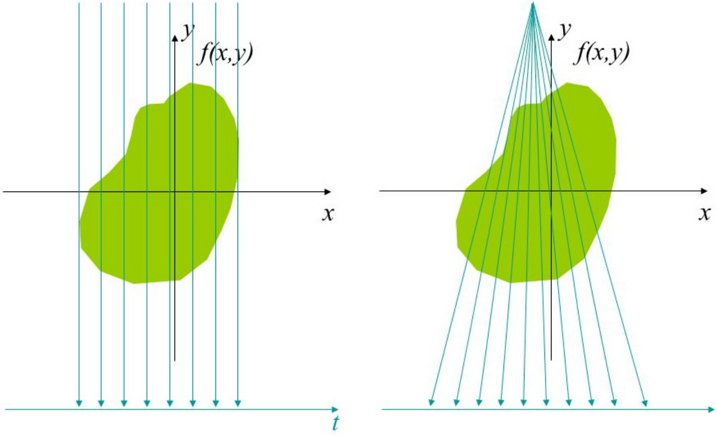

image courtesy of Gillian Henderson

Fan-beam reconstruction

- Rays not parallel, not a Radon transform.
- Rebinning

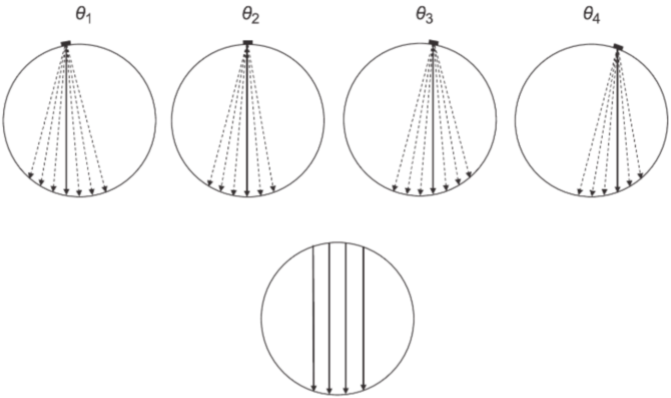

image courtesy of Jonathan Mamou and Yao Wang

Fan-beam reconstruction (2)

- Rays not parallel, not a Radon transform.
- Exact algorithms:
  - Rebinning
  - filtered backprojection (Katsevich) — computational complexity, increased dose.
- Approximate algorithms: Modified filtered backprojection (quadratic cosine correction, $\cos\theta$). Feldkamp-Davis-Kress

Fan-beam reconstruction (2)

- Rays not parallel, not a Radon transform.
- Exact algorithms:
  - Rebinning
  - filtered backprojection (Katsevich) — computational complexity, increased dose.
- Approximate algorithms: Modified filtered backprojection (quadratic cosine correction, $\cos\theta$). Feldkamp-Davis-Kress
- Algebraic reconstruction. Best quality but slow.

Analytical methods

Algebraic reconstruction

3D CT

Radiation dose

Algebraic reconstruction

- Setup and solve a (large) system of equations describing the measurements.
- Mostly (but not necessarily) linear

Algebraic reconstruction

- Setup and solve a (large) system of equations describing the measurements.
- Mostly (but not necessarily) linear

Advantages over FBP

- Better modeling of the physics — attenuation, scattering, limited resolution, beam geometry, sensor noise, beam hardening...
- Flexible, better handling of limited acquisition — restricted region, restricted angles, few measurements required
- Can use a statistical image model (regularization)
- Higher quality, less apparent artifacts

Disadvantage — speed

FBP versus ART

few projections

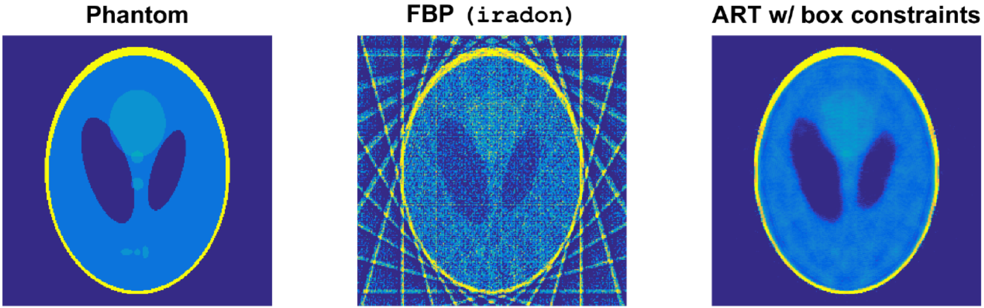

Courtesy of Technical University of Denmark

FBP versus ART

missing angles

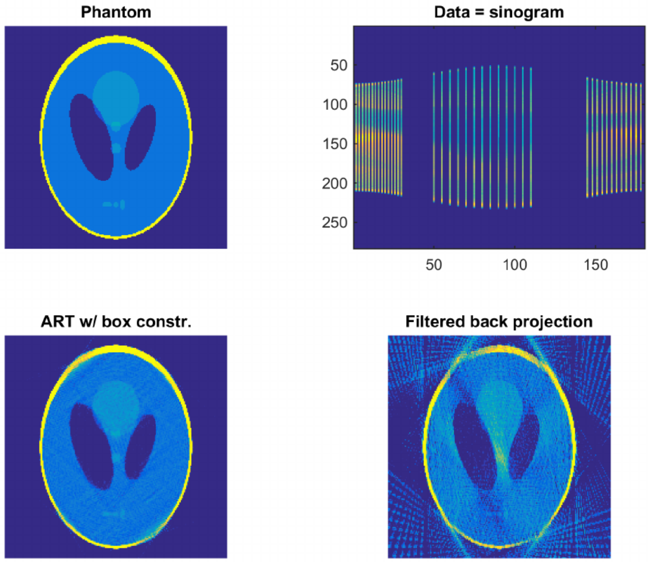

Courtesy of Technical University of Denmark

Linear reconstruction

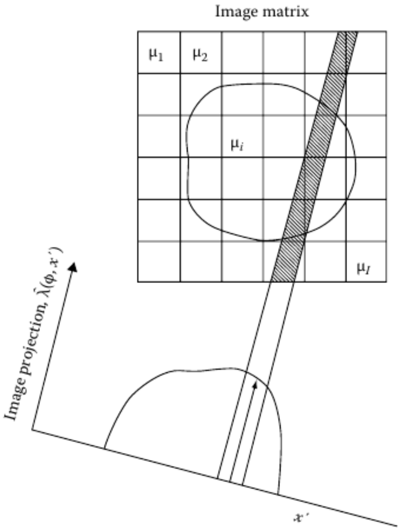

Linear reconstruction

- Discretize continuous $\mu(\mathbf{x})$ to pixels μ_i

$$\mu(\mathbf{x}) = \sum_{i=1}^{M} \mu_i \psi_i(\mathbf{x})$$

- Basis functions (piecewise constant, P0)

$$\psi_i(\mathbf{x}) = \begin{cases} 1, \text{if } \mathbf{x} \text{ in pixel } i \\ 0, \text{otherwise} \end{cases}$$

Linear reconstruction

- Discretize continuous $\mu(\mathbf{x})$ to pixels μ_i

$$\mu(\mathbf{x}) = \sum_{i=1}^{M} \mu_i \psi_i(\mathbf{x})$$

- Basis functions (piecewise constant, P0)

$$\psi_i(\mathbf{x}) = \begin{cases} 1, \text{if } \mathbf{x} \text{ in pixel } i \\ 0, \text{otherwise} \end{cases}$$

- Radon transform

$$P_\varphi(r) = \mathscr{R}\left[\mu\right](\varphi, r) = \sum_{i=1}^{M} \mu_i \mathscr{R}\left[\psi_i\right](\varphi, r)$$

Linear reconstruction (2)

- For all projections $p_j = P_{\varphi_j}(r_j)$, $j = 1, \ldots, N$

$$p_j = P_{\varphi_j}(r_j) = \sum_{i=1}^{M} \mu_i \underbrace{\mathscr{R}[\psi_i](\varphi_j, r_j)}_{w_{ij}}$$

$$p_j = \sum_{i=1}^{M} w_{ij} \mu_i$$

$$\mathbf{p} = \mathrm{W}\boldsymbol{\mu}$$

where μ_i are pixel values, p_j are the projections.

Knowing $\mathbf{p}$, solve for $\boldsymbol{\mu}$.

Linear reconstruction (2)

- For all projections $p_j = P_{\varphi_j}(r_j)$, $j = 1, \ldots, N$

$$p_j = P_{\varphi_j}(r_j) = \sum_{i=1}^{M} \mu_i \underbrace{\mathscr{R}[\psi_i](\varphi_j, r_j)}_{w_{ij}}$$

$$p_j = \sum_{i=1}^{M} w_{ij} \mu_i$$

$$\mathbf{p} = \mathrm{W} \boldsymbol{\mu}$$

  where μ_i are pixel values, p_j are the projections.

  Knowing $\mathbf{p}$, solve for $\boldsymbol{\mu}$.

- Linear equation system
  - is big ($10^4 \sim 10^6$ unknowns and measurements)
  - can be overdetermined
  - can be underdetermined
  - is sparse

Weight coefficients

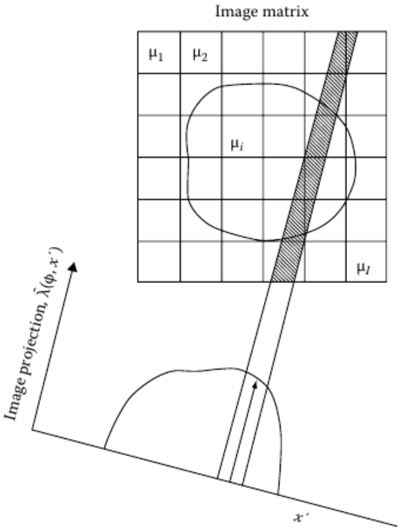

Weight coefficients

For line rays — intersection length

$$w_{ij} = \int\limits_{\mathbf{x} \in L(r_j, \varphi_j)} \psi_i(\mathbf{x}) \mathrm{d}l$$

For thick rays — intersection area

$$w_{ij} = \int\limits_{\mathbf{x} \in L'(r_j, \varphi_j)} \psi_i(\mathbf{x}) \mathrm{d}\mathbf{x}$$

Weight coefficients

For line rays — intersection length

$$w_{ij} = \int_{\mathbf{x} \in L(r_j, \varphi_j)} \psi_i(\mathbf{x}) \mathrm{d}l$$

Binary approximation

$$w_{ij} = \begin{cases} 1, & \text{if ray } L(r_j, \varphi_j) \text{ intersects pixel } \psi_i \\ 0, & \text{otherwise} \end{cases}$$

Least squares solution

for overdetermined systems

Minimize the reconstruction error $\mathbf{e}$

$$\boldsymbol{\mu}^* = \arg\min_{\boldsymbol{\mu}} \|\underbrace{\mathrm{W}\boldsymbol{\mu} - \mathbf{p}}_{\mathbf{e}}\|^2$$

Least squares solution

for overdetermined systems

Minimize the reconstruction error **e**

$$\boldsymbol{\mu}^* = \arg\min_{\boldsymbol{\mu}} \|\underbrace{\mathsf{W}\boldsymbol{\mu} - \mathbf{p}}_{\mathbf{e}}\|^2$$

The reconstruction error **e** must be perpendicular to *range* of W.

$$0 = \mathsf{W}^T\mathbf{e} = \mathsf{W}^T(\mathsf{W}\boldsymbol{\mu}^* - \mathbf{p})$$

Normal equations

$$\mathsf{W}^T\mathbf{p} = \mathsf{W}^T\mathsf{W}\boldsymbol{\mu}^*$$

Pseudoinverse solution

$$\boldsymbol{\mu}^* = (\mathsf{W}^T\mathsf{W})^{-1}\mathsf{W}^T\mathbf{p}$$

suitable for smaller problems

Minimum-norm solution

for underdetermined systems or noisy data

Add regularization D

$$\boldsymbol{\mu}^* = \arg\min_{\boldsymbol{\mu}} \|\underbrace{\mathrm{W}\boldsymbol{\mu} - \mathbf{p}}_{\mathbf{e}}\|^2 + \lambda \|\mathrm{D}\boldsymbol{\mu}\|^2$$

Normal equations

$$\mathrm{W}^T\mathbf{p} = \left(\mathrm{W}^T\mathrm{W} + \lambda \mathrm{D}^T\mathrm{D}\right)\boldsymbol{\mu}^*$$

Pseudoinverse solution

$$\boldsymbol{\mu}^* = \left(\mathrm{W}^T\mathrm{W} + \lambda \mathrm{D}^T\mathrm{D}\right)^{-1}\mathrm{W}^T\mathbf{p}$$

Iterative methods

Principles

- Start from an initial guess of $\boldsymbol{\mu}$
- Compare measured projections and simulations
- Correct pixel values to decrease the difference
- Iterate until convergence

Properties

- Take advantage of the sparseness (complexity $O(N)$ per iteration)
- Low memory complexity ($O(M)$)
- $\longrightarrow$ Suitable for large systems of equations
- Early stopping
- Slower for small problems (compared to direct methods)

Projection method

Kaczmarz's method

$$p_j = \sum_{i=1}^{M} w_{ij}\mu_i, \qquad j = 1, 2, \ldots, N$$

$$p_j = \langle \mathbf{w}_j, \boldsymbol{\mu} \rangle = \mathbf{w}_j^T \boldsymbol{\mu}$$

Projection method

Kaczmarz's method

$$p_j = \sum_{i=1}^{M} w_{ij}\mu_i, \qquad j = 1, 2, \ldots, N$$

$$p_j = \langle \mathbf{w}_j, \boldsymbol{\mu} \rangle = \mathbf{w}_j^T \boldsymbol{\mu}$$

- Affine solution space of equation j

$$\mathcal{S}_j = \{\boldsymbol{\mu} \in \mathbb{R}^M ; p_j = \langle \mathbf{w}_j, \boldsymbol{\mu} \rangle\}$$

Normal vector $\mathbf{w}_j$

$$\forall \boldsymbol{\mu} \in \mathcal{S}_j, \boldsymbol{\mu}' \in \mathcal{S}_j;\ \langle \mathbf{w}_j, \boldsymbol{\mu} - \boldsymbol{\mu}' \rangle = 0$$

Projection to an affine space

"affine space is a geometric structure that generalizes some of the properties of Euclidean spaces in such a way that these are independent of the concepts of distance and measure of angles, keeping only the properties related to parallelism and ratio of lengths for parallel line segments."

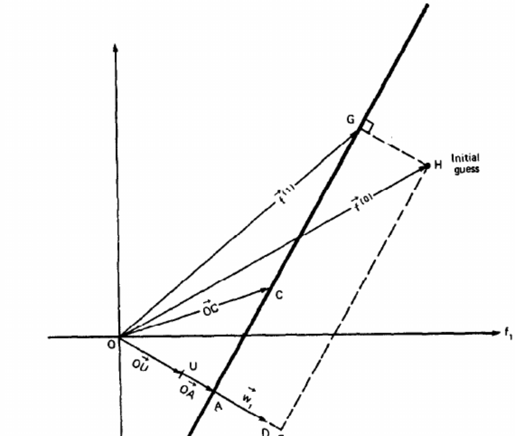

Projection to an affine space

”affine space is a geometric structure that generalizes some of the properties of Euclidean spaces in such a way that these are independent of the concepts of distance and measure of angles, keeping only the properties related to parallelism and ratio of lengths for parallel line segments.”

Projection onto $\mathcal{S}_j$

$$\mathbf{g}^* = \mathcal{P}_{\mathcal{S}_j}(\mathbf{h}) = \arg\min_{\mathbf{g}\in\mathcal{S}_j} \|\mathbf{g} - \mathbf{h}\|$$

Moving in the normal direction (minimum change) until hitting $\mathcal{S}_j$

$$\mathbf{g}^* = \mathbf{h} - \lambda \mathbf{w}_j$$
$$p_j = \langle \mathbf{w}_j, \mathbf{h} \rangle$$

Solution

$$\lambda = (\langle \mathbf{w}_j, \mathbf{h} \rangle - p_j)/(\langle \mathbf{w}_j, \mathbf{w}_j \rangle) \qquad \text{normalized residual}$$
$$\mathbf{g}^* = \mathbf{h} - (\langle \mathbf{w}_j, \mathbf{h} \rangle - p_j)(/\langle \mathbf{w}_j, \mathbf{w}_j \rangle \mathbf{w}_j)$$

Projection method

the algorithm

- Initial solution $\boldsymbol{\mu}^{(0)}$ (e.g. random)
- Project sequentially to constraints $1, 2, \ldots, N, 1, 2, \ldots$

$$\boldsymbol{\mu}^{(1)} = \mathcal{P}_{\mathcal{S}_1} \boldsymbol{\mu}^{(0)}$$
$$\boldsymbol{\mu}^{(2)} = \mathcal{P}_{\mathcal{S}_2} \boldsymbol{\mu}^{(1)}$$
$$\boldsymbol{\mu}^{(3)} = \mathcal{P}_{\mathcal{S}_3} \boldsymbol{\mu}^{(3)}$$
$$\ldots$$

- Repeat until convergence

Interpretation of the update

$$\boldsymbol{\mu}^{(k+1)} = \boldsymbol{\mu}^{(k)} - \underbrace{\frac{\langle \mathbf{w}_j, \boldsymbol{\mu}^{(k)} \rangle - p_j}{\langle \mathbf{w}_j, \mathbf{w}_j \rangle}}_{\tilde{p}_j} \mathbf{w}_j$$

$$p_j = \sum_{i=1}^{M} w_{ij} \mu_i = \langle \mathbf{w}_j, \boldsymbol{\mu} \rangle$$

Projection $\hat{p}_j \langle \mathbf{w}_j, \boldsymbol{\mu}^{(k)} \rangle$ along ray j
Backprojection of the correction $\tilde{p}_j$ along ray j

Projection

$N = 2$

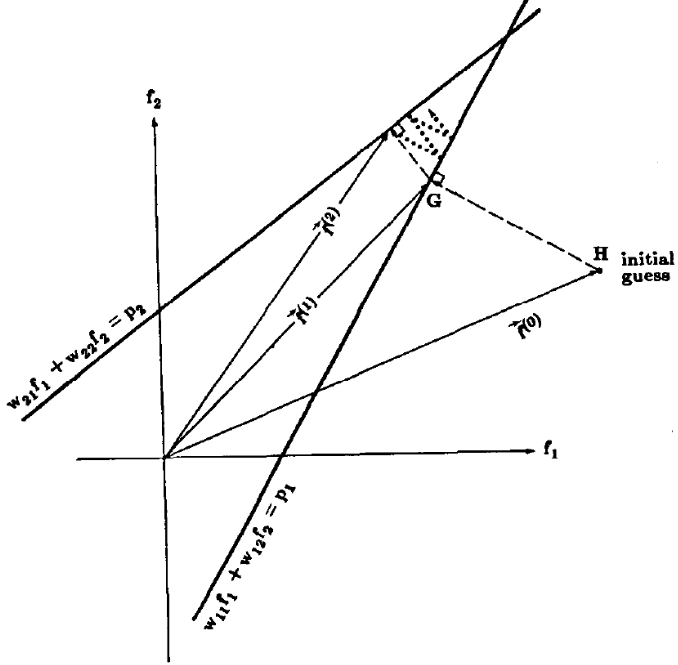

Projection method

properties

- Computationally cheap: one projection cost $O(M)$, applying all constraints $O(MN)$
- Low-memory complexity: $O(M)$ if $\mathbf{w}_{ij}$ can be calculated on the fly.
- If a solution exists, the projection method converges to it.
- Convergence may be slow.
- If no solution exists, the method may oscillate.

Projection method improvements

- Constraint ordering

Projection method improvements

- Constraint ordering
- Under/overrelaxation,

$$\boldsymbol{\mu} = \boldsymbol{\mu}^{(0)} - \alpha \frac{\langle \mathbf{w}_j, \boldsymbol{\mu} \rangle - p_j}{\langle \mathbf{w}_j, \mathbf{w}_j \rangle} \mathbf{w}_j$$

$$0 < \alpha < 2$$

Projection method improvements

- Constraint ordering
- Under/overrelaxation,

$$\boldsymbol{\mu} = \boldsymbol{\mu}^{(0)} - \alpha \frac{\langle \mathbf{w}_j, \boldsymbol{\mu} \rangle - p_j}{\langle \mathbf{w}_j, \mathbf{w}_j \rangle} \mathbf{w}_j$$

$$0 < \alpha < 2$$

- Incorporating constraints — positivity ($\mu_i \geq 0$), zero outside,. . .

Simplified update rules

- Binary additive case ($w_{ij} \in \{0, 1\}$)

$$\forall j,\ g_k^* = h_k - \frac{\sum\limits_{i, w_{ij}=1} h_i - p_j}{N_j}, \qquad \text{for } w_{kj} = 1,\ N_j = \sum_i w_{ij} = 1$$

- Binary multiplicative case ($w_{ij} \in \{0, 1\}$)

$$\forall j,\ g_k^* = h_k \frac{p_k}{\sum\limits_{i, w_{ij}=1} h_i}, \qquad \text{for } w_{kj} = 1$$

Projections by integration

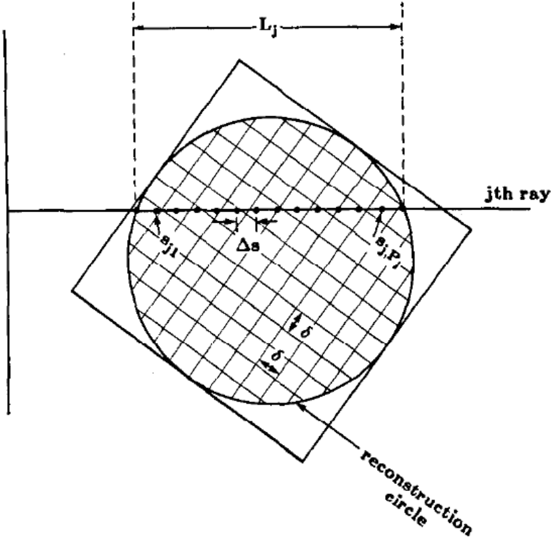

Projections by integration

$$p_j = \int \mu(r_j \cos\varphi_j - t\sin\varphi, r_j \sin\varphi_j + t\cos\varphi)\mathrm{d}t$$

$$p_j = \sum_{i=1}^{M} w_{ij}\mu_i = \langle \mathbf{w}_j, \boldsymbol{\mu} \rangle$$

$$\mu(\mathbf{x}) = \sum_{i=1}^{M} \mu_i \psi_i(\mathbf{x})$$

$$w_{ij} = \int \psi_i(r_j \cos\varphi_j - t\sin\varphi, r_j \sin\varphi_j + t\cos\varphi)\mathrm{d}t$$

$$p_j = \Delta s \sum_k \mu(r_j \cos\varphi_j - t\sin\varphi, r_j \sin\varphi_j + t\cos\varphi),$$

with $t = \Delta s\, k$

Backprojections by integration

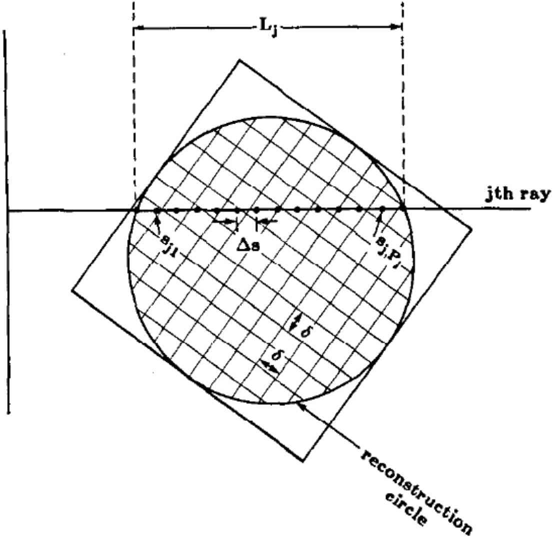

Other iterative methods

- simultaneous iterative reconstruction (SIRT), Cimmino's method — block update
- simultaneous algebraic reconstruction technique (SART) — bilinear ψ, projection by integration, Hamming window over rays
- iterative least-squares technique (ILST)
- multiplicative algebraic reconstruction technique (MART)
- iterative sparse asymptotic minimum variance (SAMV)
- (preconditioned) conjugated gradients (CG) — with regularization for ill-posed problems
- ...

Example

moving heart

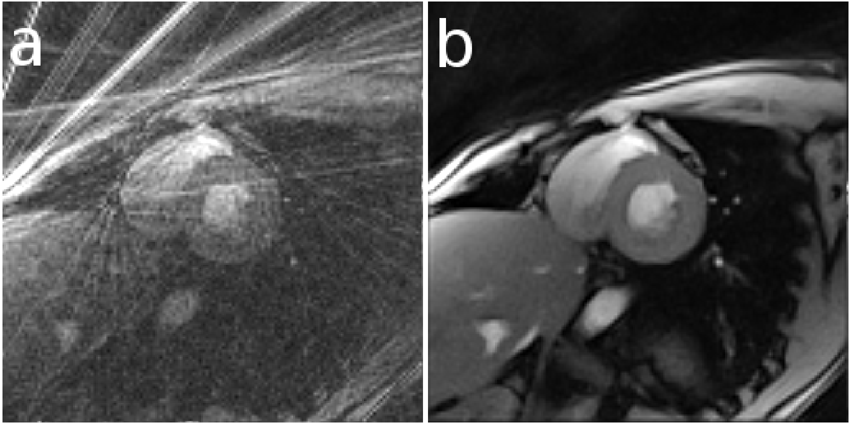

filtered back projection iterative (nonlinear)

Courtesy of Biomedizinische NMR Forschungs GmbH

Analytical methods

Algebraic reconstruction

3D CT

Radiation dose

3D computed tomography

- Technical challenges: power, cooling
- Rotation method (slice by slice)
- Spiral/helix method

Spiral method

- Acceleration: 10 min → 1 min

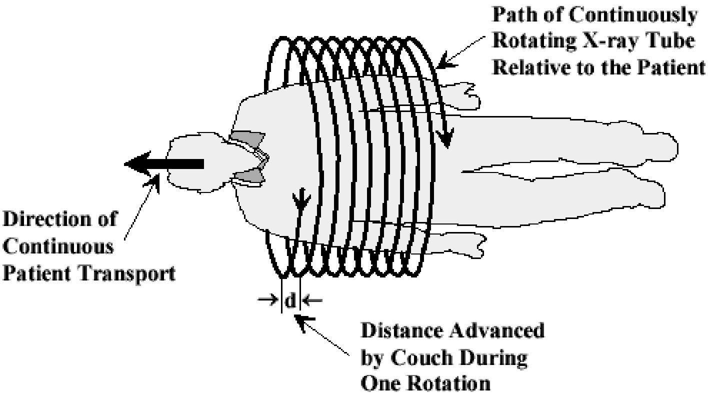

Spiral method

- Acceleration: 10 min $\to$ 1 min
- *Pitch*:

$$P = \Delta l / d$$

Δl bed shift per rotation, d slice thickness.
Normally $0 < P < 2$. Overlap for $P < 1$. Typically $P = 1.5$.

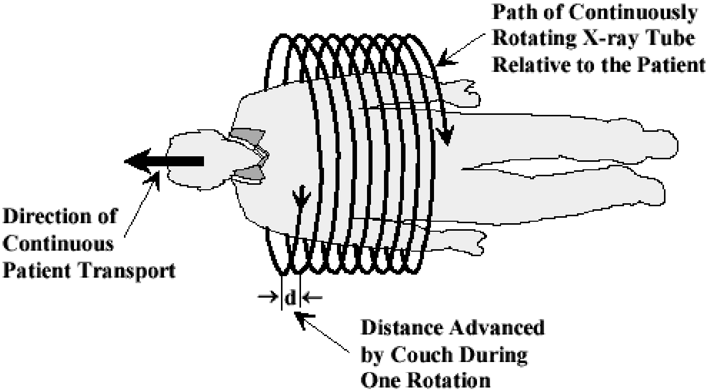

Spiral method (2)

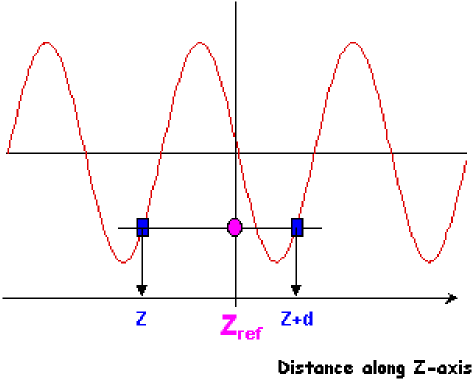

- Interpolation in z axis
- Interpolation *wide* — 1 turn. Less noise, larger effective slice thickness.
- Interpolation *Slim* — $1/2$ turn, symmetry. More noise, smaller effective slice thickness.

Spiral method (2)

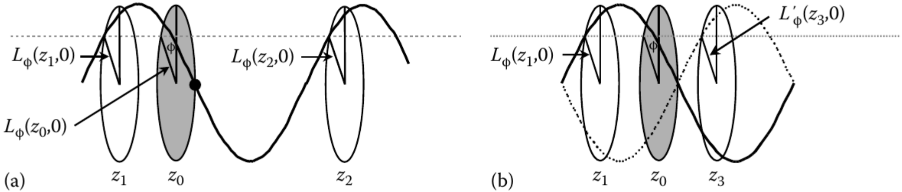

- Interpolation in z axis
- Interpolation *wide* — 1 turn. Less noise, larger effective slice thickness.
- Interpolation *Slim* — $1/2$ turn, symmetry. More noise, smaller effective slice thickness.

Multislice acquisition

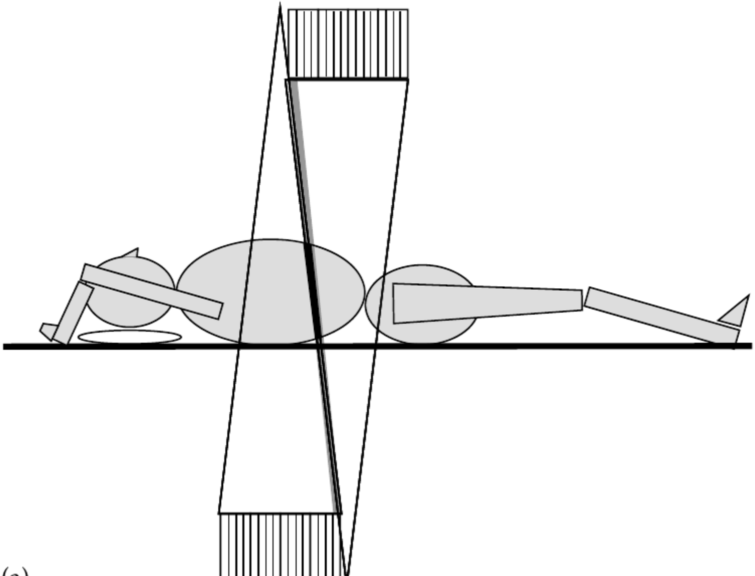

Multislice acquisition

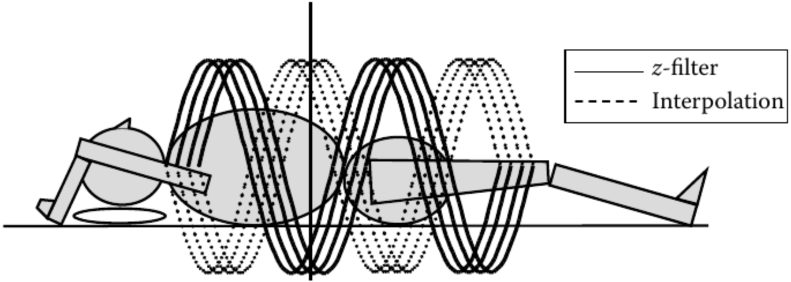

- Multi-plane reconstruction / multi-slice linear interpolation / multi-slice filtered interpolation

Multislice acquisition

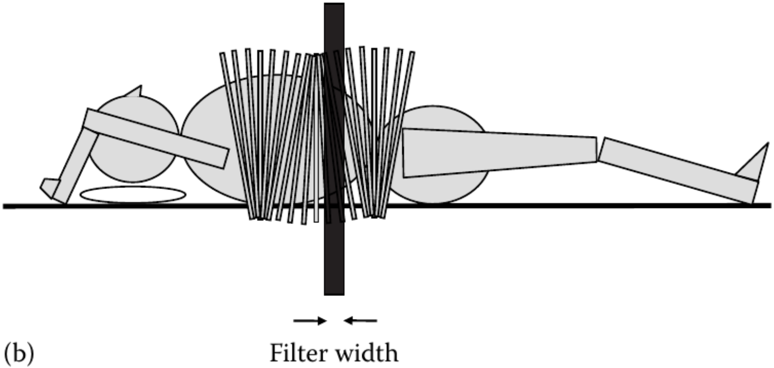

- Multi-plane reconstruction / multi-slice linear interpolation / multi-slice filtered interpolation

CT image quality

- Parameters:
  - Resolution (0.5 mm)
  - Contrast (δH, about $5 - 10$ HU.)
  - Detection threshold (about 1 mm at $\Delta H = 200$, 5 mm at $\Delta H = 5$).
  - Noise (SNR)
- Artifacts
  - Scanner defects, malfunctions, operator error
  - Metal parts (shadows)
  - Motion artifacts
  - Partial volume

Artifact examples

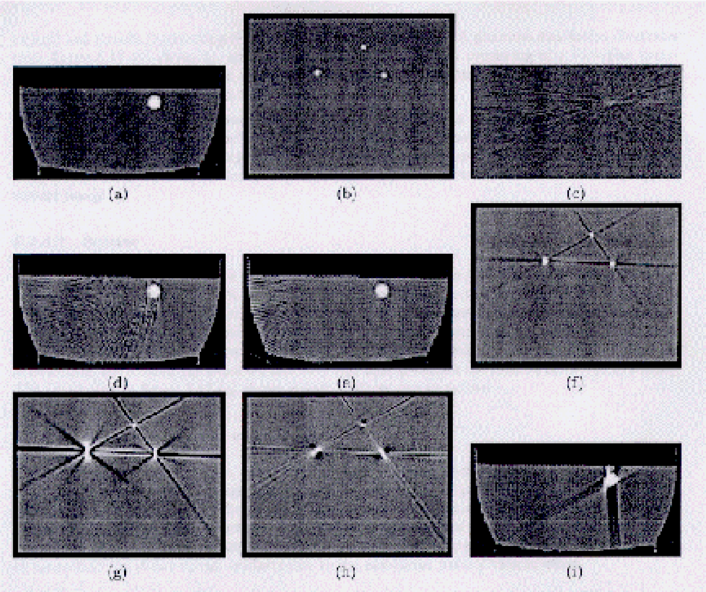

Analytical methods

Algebraic reconstruction

3D CT

Radiation dose

Radiation dose

- Absorbed dose D in units $1\,\mathrm{Gy}$ (gray) $= 1\,\mathrm{J/kg}$.
  Before $1\,\mathrm{Gy} = 100\,\mathrm{rad}$
- Effective dose equivalent (dávkový ekvivalent) H_E [Sv] (sievert)

  $$H_\mathrm{E} = \sum_i w_i H_i = \sum_i w_i c_i D_i$$

  $H = cD$. Quality factor c is 1 for X-rays and γ rays, 10 for neutrons, 20 for α particles.

  Coefficient w is organ dependent: male/female glands 0.2, lungs 0.12, breast 0.1, stomach 0.12, thyroid gland 0.05, skin 0.01. $\sum w_i = 1$.
  Before $1\,\mathrm{Sv} = 100\,\mathrm{rem}$

Radiation dose

- Absorbed dose D in units $1\,\mathrm{Gy}$ (gray) $= 1\,\mathrm{J/kg}$.
  Before $1\,\mathrm{Gy} = 100\,\mathrm{rad}$
- Effective dose equivalent (dávkový ekvivalent) H_E [Sv] (sievert)

  $$H_\mathrm{E} = \sum_i w_i H_i = \sum_i w_i c_i D_i$$

  $H = cD$. Quality factor c is 1 for X-rays and γ rays, 10 for neutrons, 20 for α particles.

  Coefficient w is organ dependent: male/female glands 0.2, lungs 0.12, breast 0.1, stomach 0.12, thyroid gland 0.05, skin 0.01. $\sum w_i = 1$.
  Before $1\,\mathrm{Sv} = 100\,\mathrm{rem}$
- Sum the doses

Radiation dose

- Medical limit (USA) is 50 mSv/year
  (limit for a person working with radiation),
  corresponding to 1000 chest X-rays,
  or 15 head CTs,
  or 5 whole body CTs (1 CT$\approx$ 10 mSv).
- low-dose CT$\approx 2 \sim 5$ mSv, PET$\approx$ 25 mSv
- In radioactive background about 3 mSv/year (mainly radon).
  In Colorado (altitude $1500 \sim 4000$ m) about 4.5 mSv/year. Mean dose from medical imaging 0.3 mSv/year,
  about 3 long flights.
- aircrew members have the largest average annual effective dose about 3 mSv of all US radiation-exposed workers.
  Reason: galactic cosmic radiation, which is always present, and
  solar particle events, called "solar flares"

Radiation dose

- Medical limit (USA) is 50 mSv/year
  (limit for a person working with radiation),
  corresponding to 1000 chest X-rays,
  or 15 head CTs,
  or 5 whole body CTs (1 CT$\approx$ 10 mSv).
- low-dose CT$\approx 2 \sim 5$ mSv, PET$\approx$ 25 mSv
- In radioactive background about 3 mSv/year (mainly radon).
  In Colorado (altitude $1500 \sim 4000$ m) about 4.5 mSv/year. Mean dose from medical imaging 0.3 mSv/year,
  about 3 long flights.
- aircrew members have the largest average annual effective dose about 3 mSv of all US radiation-exposed workers.
  Reason: galactic cosmic radiation, which is always present, and
  solar particle events, called "solar flares"
- cancer related death 20 %. 1 CT=10 mSv — relative increase by $10^{-3} \sim 10^{-4}$

Computed Tomography, conclusions

- Excellent spatial resolution
- 3D image
- Fast acquisition
- Weak soft tissue contrast (contrast agents available)
- Reconstruction algorithm
- Radiation dose